# Phase Coherence of an Atomic Mott Insulator

Fabrice Gerbier, Artur Widera, Simon Fölling, Olaf Mandel, Tatjana Gericke, and Immanuel Bloch
*Institut für Physik, Johannes Gutenberg-Universität, 55099 Mainz, Germany*
(Received 17 March 2005; published 28 July 2005)

We investigate the phase coherence properties of ultracold Bose gases in optical lattices, with special emphasis on the Mott insulating phase. We show that phase coherence on short length scales persists even deep in the insulating phase, preserving a finite visibility of the interference pattern observed after free expansion. This behavior can be attributed to a coherent admixture of particle-hole pairs to the perfect Mott state for small but finite tunneling. In addition, small but reproducible kinks are seen in the visibility, in a broad range of atom numbers. We interpret them as signatures for density redistribution in the shell structure of the trapped Mott insulator.

DOI: 10.1103/PhysRevLett.95.050404 PACS numbers: 03.75.Lm, 03.75.Gg, 03.75.Hh

A fundamental aspect of ultracold bosonic gases is their phase coherence. The existence of long-range phase coherence, inherent to the description of a Bose-Einstein condensate in terms of a coherent matter wave, was experimentally demonstrated in interferometric [1–3] or spectroscopic [4] experiments. More recently, attention has been paid to fundamental mechanisms that may degrade or even destroy long-range coherence, for example, thermal phase fluctuations in elongated condensates [5–8], or the superfluid to Mott insulator (MI) transition undergone in optical lattices [9–11].

For a Bose-Einstein condensate released from an optical lattice, the density distribution after expansion shows a sharp interference pattern [10]. In a perfect Mott insulator, where atomic interactions pin the density to precisely an integer number of atoms per site, phase coherence is completely lost and no interference pattern is expected. The transition between these two limiting cases happens continuously as the lattice depth is increased. In the superfluid phase, a partial loss of long-range coherence due to an increased quantum depletion has been observed for lattice depths below the MI transition [12–14]. Conversely, in the insulating phase, numerical simulations [15–17] and experiments [10,18]indicate a residual interference, although *long-range* coherence and superfluidity have vanished.

In this Letter, we revisit this question of phase coherence focusing on the insulating phase. We observe that the interference pattern persists in the MI phase, and that its visibility decays rather slowly with increasing lattice depth. We explain this behavior as a manifestation of short-range coherence in the insulating phase, fundamentally due to a coherent admixture of particle-hole pairs to the ground state for large but finite lattice depths. In addition, we also observe reproducible ''kinks'' in the visibility at well-defined lattice depths. We interpret them as a signature of density redistribution in the shell structure of a MI in an inhomogeneous potential, when regions with larger-than-unity filling form. Finally, the issue of adiabatic loading in the lattice is briefly discussed.

In our experiment, a $^{87}$Rb Bose-Einstein condensate is loaded into an optical lattice created by three orthogonal pairs of counterpropagating laser beams (see [10] for more details). The superposition of the lattice beams, derived from a common source at a wavelength $\lambda_L = 850$ nm, results in a simple cubic periodic potential with a lattice spacing $d = \lambda_L/2 = 425$ nm. The lattice depth $V_0$ is controlled by the laser intensities, and is measured here in units of the single-photon recoil energy, $E_R = h^2/2m\lambda_L^2 \approx h \times 3.2$ kHz, where $m$ is the atomic mass. The optical lattice is ramped up in 160 ms, using a smooth waveform that minimizes sudden changes at both ends of the ramp. After switching off the optical and magnetic potentials simultaneously and allowing for typically $t = 10$–$22$ ms of free expansion, standard absorption imaging of the atom cloud yields a two-dimensional map of the density distribution (integrated along the probe line of sight).

Four such images are shown in Figs. 1(a)–1(d), for various lattice depths. The density distribution of these expanding clouds can be expressed as [15,16,19]

$$n(\mathbf{r}) = \left(\frac{m}{\hbar t}\right)^3 \left| \tilde{w}\left(\mathbf{k} = \frac{m\mathbf{r}}{\hbar t}\right) \right|^2 S\left(\mathbf{k} = \frac{m\mathbf{r}}{\hbar t}\right). \quad (1)$$

In Eq. (1), the interference pattern is described by

$$S(\mathbf{k}) = \sum_{i,j} e^{i\mathbf{k}\cdot(\mathbf{r}_i - \mathbf{r}_j)} \langle \hat{a}_i^\dagger \hat{a}_j \rangle, \quad (2)$$

where the operator $\hat{a}_i^\dagger$ creates an atom at site $i$, and where

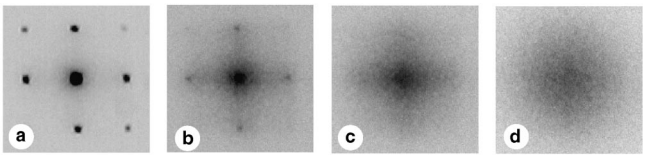


FIG. 1. Absorption images of an ultracold Bose gas released from an optical lattice, for various lattice depths: (a) $8E_R$, (b) $14E_R$, (c) $18E_R$, and (d) $30E_R$.

 

$\tilde{w}$ is the Fourier transform of the Wannier function $w(\mathbf{r}_i)$. The Fourier relation (2) shows that long-range phase coherence, i.e., a correlation function $\langle \hat{a}_i^\dagger \hat{a}_j \rangle$ slowly varying across the lattice, is necessary to observe a sharp diffraction pattern as in Fig. 1(a). However, above the MI transition [Figs. 1(b)–1(d)], the interference peaks evolve into a much broader, crosslike structure that weakens with increasing lattice depth. This slow modulation corresponds to short-range coherence, i.e., a correlation function $\langle \hat{a}_i^\dagger \hat{a}_j \rangle$ whose range extends over a few sites only.

To extract quantitative information from time-of-flight pictures as shown in Fig. 1, Eq. (1) suggests using the usual definition of the visibility of interference fringes,

$$\mathcal{V} = \frac{n_{\max} - n_{\min}}{n_{\max} + n_{\min}} = \frac{S_{\max} - S_{\min}}{S_{\max} + S_{\min}}. \tag{3}$$

In this work, we measure the maximum density $n_{\max}$ at the first lateral peaks of the interference pattern [20], (i.e., at the center of the second Brillouin zone), whereas the minimum density $n_{\min}$ is measured along a diagonal with the same distance from the central peak [see inset in Fig. 2(a)]. In this way, the Wannier envelope is the same for each term and cancels out in the division, yielding the contrast of $S$ alone [hence the second equality in Eq. (3)]. Four pairs exist for a given absorption image, and their values are averaged to yield the visibility. In previous studies of the MI transition [10,14], the sharpness of the interference pattern was characterized by the half-width of the central peak. Such a measure is possibly sensitive to systematic effects, such as optical saturation and mean-field broadening. We expect our measure of contrast to be much less sensitive to these effects, since it is calculated in regions of the image where the density is lower.

We present here measurements of the visibility as a function of lattice depth (typically in a range $(6\text{–}30)E_R$) at a given total atom number. Each value was obtained as the visibility averaged over approximately 10 independent images. Different atom numbers (hence different filling factors) were investigated, ranging from $6 \times 10^4$ to $6 \times 10^5$. Two illustrative sets of data are shown in Fig. 2, corresponding to approximately $5.9 \times 10^5$ atoms (black circles) and $3.6 \times 10^5$ atoms (gray circles). For lattice depths larger than $12.5E_R$, the system is in the insulating phase [10]. Yet, the visibility remains finite well above this point. For example, at a lattice depth of $15E_R$, the contrast is still around 30%, reducing to a few percent level only for a rather high lattice depth of $30E_R$. We now show that such a slow loss in visibility is expected in the ground state of the system.

As shown in [9], the physics of ultracold atoms in an optical lattice can be described by the Bose-Hubbard Hamiltonian, given by the sum of a tunneling term, $\mathcal{H}_t = -t\Sigma_{\langle i,j \rangle} \hat{a}_i^\dagger \hat{a}_j$, plus an interaction term, $\mathcal{H}_{\text{int}} = \Sigma_i \frac{U}{2} \hat{n}_i(\hat{n}_i - 1)$. Here $\hat{n}_i = \hat{a}_i^\dagger \hat{a}_i$ is the on-site number operator, $t$ is the tunneling matrix element, the notation $\langle i, j \rangle$ restricts the sum to nearest neighbors only, and $U$ is the on-site interaction energy [11]. In the experiments, an additional, slowly varying potential $V_{\text{ext}}(\mathbf{r})$ is also present and favors the formation of a "wedding cake" structure of alternating MI and superfluid shells [9,15,21], which reflects the characteristic lobes delimiting the MI phases in the phase diagram of the Bose-Hubbard model [11].

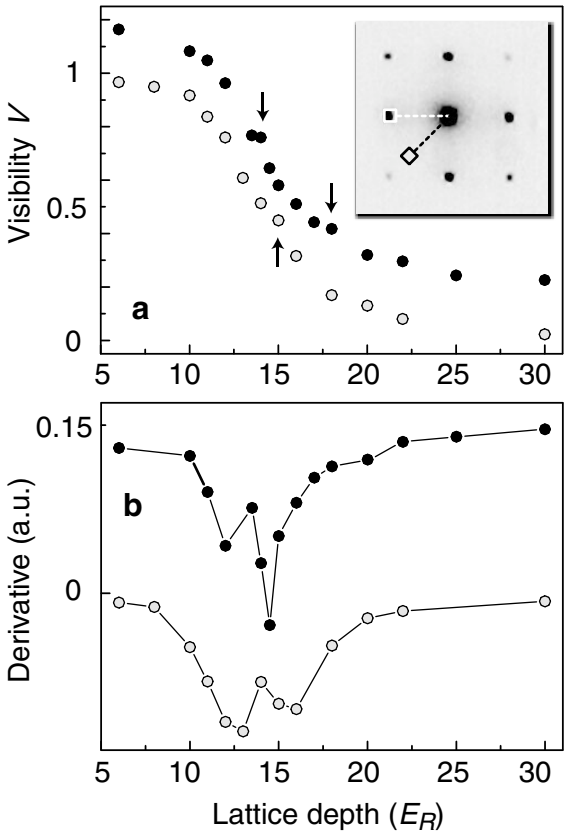


FIG. 2. (a) Visibility of the interference pattern produced by an ultracold cloud released from an optical lattice. The two sets of data shown correspond to $3.6 \times 10^5$ atoms (gray circles) and $5.9 \times 10^5$ atoms (black circles). The latter curve has been offset vertically for clarity. Arrows mark positions where kinks are visible. (b) Numerical derivative of the above curves.

To better understand the origin of a finite visibility, we consider a homogeneous system with filling factor $n_0$. In the limit of infinitely strong repulsion, $U/t \to \infty$, the ground state is what we call a "perfect" Mott insulator, i.e., a uniform array of Fock states, $|\Psi\rangle_{\text{MI}} = \prod_i |n_0\rangle_i$. This corresponds to a uniform $S = n_0$ and zero visibility. To a good approximation, the actual ground state for a finite ratio $U/t$ can be calculated by considering the tunneling term as a perturbation to the interaction term. To first order in $t/U$, this yields

$$|\Psi^{(1)}\rangle \approx |\Psi\rangle_{\text{MI}} + \frac{t}{U} \sum_{\langle i,j \rangle} \hat{a}_i^\dagger \hat{a}_j |\Psi\rangle_{\text{MI}}. \tag{4}$$

The ground state thus acquires a small admixture of

''particle-hole'' pairs (i.e., an additional particle at one lattice site and a missing one in a neighboring site), which restores short-range coherence and a corresponding weak modulation in the momentum distribution, $S(\mathbf{k}) \propto n_0 - 2n_0(n_0+1)t(\mathbf{k})/U$, where $t(\mathbf{k}) = -2t\Sigma_{\nu=x,y,z}\cos(k_\nu d)$ is the tight-binding dispersion relation. The corresponding 2D visibility (integrated along one direction) is

$$\mathcal{V} \approx \frac{4}{3}(n_0+1)\frac{zt}{U}. \quad (5)$$

In Eq. (5), $z = 6$ is the number of nearest neighbors in a 3D cubic lattice.

To compare with the experiment, we show in Fig. 3 the visibility against $U/zt$ in a log-log plot. For lattice depths $V_0 \geq 14E_R$ (corresponding to $U/zt \geq 8$), the data match the inverse law expected from Eq. (5). This has been verified by fitting the data in this range to a general power law $A(U/zt)^\alpha$ (solid lines in Fig. 3). We obtain an average exponent $\alpha = -0.98(7)$ in agreement with the prediction [see Fig. 4(a)]. In Fig. 4(b), the fitted prefactor is plotted as a function of atom number. Inspired by Eq. (5), we compare it to $4(\bar{n}+1)/3$, where $\bar{n}$ is the average filling factor calculated at a lattice depth of $30E_R$ using a mean-field approximation [22,23]. We find that this extrapolation of Eq. (5) to our trapped system indeed yields the correct order of magnitude [see Fig. 4(b)]. We thus consider the agreement between our experimental results and the simple relations derived above as conclusive evidence for the presence of particle-hole pairs, characteristic of the ground state of the Bose-Hubbard Hamiltonian.

In addition to the smooth decay discussed above, the visibility shows small kinks at specific lattice depths [indicated by arrows in Fig. 2(a)]. They are systematically observed in our data, and their positions are reproducible. In the derivative plot [Fig. 2(b)], they appear as narrow maxima on a smoother background. We obtained the kink positions by taking the middle point between two adjacent Gaussian peaks with negative amplitudes fitted to the data. The most prominent kink occurs on average for a lattice depth of $14.1(8)E_R$, with a statistical error indicated between parentheses. For the largest atom numbers ($4.2 \times 10^5$ and $6 \times 10^5$), a similar but much weaker kink is also visible around $16.6(9)E_R$ (see upper curves in Fig. 2). These values are close to $14.7E_R$ and $15.9E_R$, the lattice depths where MI regions with filling factor $n_0 = 2$ or 3 are expected to form for our parameters [23]. We thus propose that the observed kinks are linked to a redistribution in the density as the superfluid shells transform into MI regions with several atoms per site. We were recently informed that similar features were reproduced numerically for one-dimensional trapped systems with a small number of particles [24].

We have considered the dependence of the visibility on the time over which the optical lattice was ramped from zero to its final value, for a specific lattice depth of $V_0 = 10E_R$. The visibility was considerably degraded for the shortest ramp time of 20 ms, but reached a ramp-independent value for ramp times larger than $T_{ad} \sim 100$ ms (to be compared to the 160 ms time used in visibility experiments). We note that $T_{ad}$ for this lattice depth of $V_0 = 10E_R$ is significantly longer than the microscopic time scales of the system, such as the tunneling time or the trapping periods. We note also that at the largest lattice depth we use here ($V_0 = 30E_R$), the observed visi-

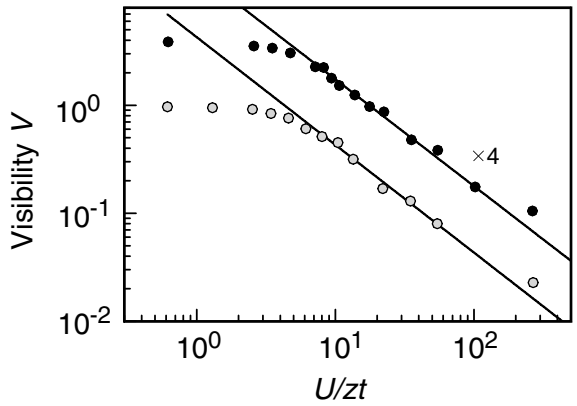


FIG. 3. Visibility of the interference pattern versus $U/zt$, the characteristic ratio of interaction to kinetic energy. The data are identical to those shown in Fig. 2 ($5.9 \times 10^5$, black circles, and $3.6 \times 10^5$ atoms, gray circles). The former curve has been offset vertically for clarity. The lines are fits to the data in the range $(14–25)E_R$, assuming a power law behavior (see text).

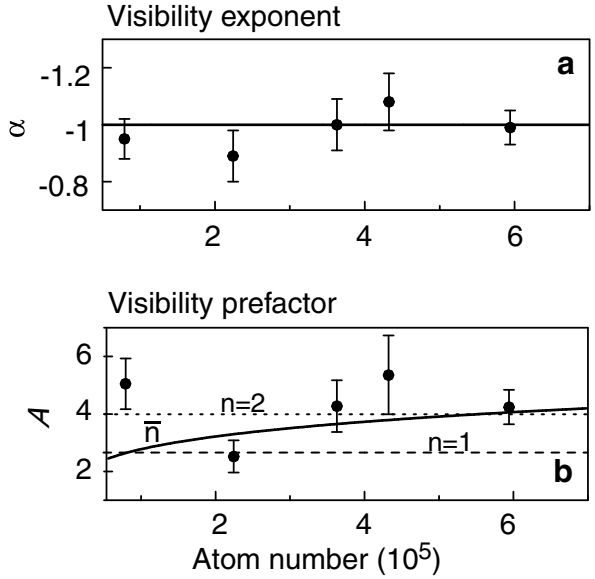


FIG. 4. Exponent $\alpha$ (a) and prefactor $A$ (b) extracted from a power law fit $A(U/zt)^\alpha$ to the visibility data in Fig. 3, plotted versus total atom number. The solid line indicates the expected exponent $\alpha = -1$. In (b), we also indicate the prefactor expected for uniform MI with filling factor $n_0 = 1$ (dashed line) and $n_0 = 2$ (dotted line), as well as an extrapolation for the average filling calculated at a lattice depth of $30E_R$ (solid line).

bility is systematically above the power law fit in Fig. 3, indicating a breakdown of adiabaticity. By comparing the data to the fitted curve, we expect this to occur for $V_0 \approx 29E_R$ ($U/zt \approx 200$), which agrees with the calculated depth of $32E_R$ for which the ramping time 160 ms becomes smaller than the calculated tunneling time $h/zt$.

Although a complete study is beyond the scope of this Letter, these observations suggest that different dynamical processes are involved in the loading, depending on whether the gas is in the superfluid or in the MI phase. In the superfluid phase, the ramp time has to be slow enough not to excite long-lived collective excitations. In the MI phase, these excitations acquire an energy gap, which makes single particle tunneling the dominant dynamical process. In this case, the final tunneling time increases with final lattice depth, and eventually becomes so long that the system basically freezes out at some lattice depth, estimated here to be $29E_R$.

In conclusion, we have studied the visibility of the interference pattern produced by an ultracold Bose gas released from a deep optical lattice. A nonvanishing visibility in the MI phase is observed and explained by the coherent admixture of particle-hole pairs to the insulating ground state, which preserves local phase coherence. This intrinsic limitation to the ''quality'' of a MI has important implications for various quantum information processing schemes, where the MI plays a central role [25–27]. In addition, we observe small but reproducible kinks in the visibility curve. We interpret them as the signature of density redistribution in the shell structure of the cloud as MI with several atoms per site are expected to form. Finally, a recent paper [28] suggests that in a planar array of one-dimensional Bose gases, the visibility might be further reduced when correlations build up in each tube, i.e., upon entering the Tonks-Girardeau regime. Experimental study of these effects seems within reach with the methods presented in this Letter.

We thank Dries van Oosten, Paolo Pedri, and Luis Santos for useful discussions. Our work is supported by the Deutsche Forschungsgemeinschaft (SPP1116), AFOSR, and the European Union under a Marie-Curie Excellence Grant. F. G. acknowledges support from a Marie-Curie Fellowship of the European Union.

[1] M. R. Andrews, C. G. Townsend, H.-J. Miesner, D. S. Durfee, D. M. Kurn, and W. Ketterle, Science **275**, 637 (1997).
[2] E. W. Hagley *et al.*, Phys. Rev. Lett. **83**, 3112 (1999).
[3] I. Bloch, T. W. Hänsch, and T. Esslinger, Nature (London) **403**, 166 (2000).
[4] J. Stenger, S. Inouye, A. P. Chikkatur, D. M. Stamper-Kurn, D. E. Pritchard, and W. Ketterle, Phys. Rev. Lett. **82**, 4569 (1999).
[5] D. S. Petrov, G. V. Shlyapnikov, and J. T. M. Walraven, Phys. Rev. Lett. **85**, 3745 (2000).
[6] S. Dettmer *et al.*, Phys. Rev. Lett. **87**, 160406 (2001).
[7] S. Richard, F. Gerbier, J. H. Thywissen, M. Hugbart, P. Bouyer, and A. Aspect, Phys. Rev. Lett. **91**, 010405 (2003).
[8] D. Hellweg, L. Cacciapuoti, M. Kottke, T. Schulte, K. Sengstock, W. Ertmer, and J. J. Arlt, Phys. Rev. Lett. **91**, 010406 (2003).
[9] D. Jaksch, C. Bruder, J. I. Cirac, C. W. Gardiner, and P. Zoller, Phys. Rev. Lett. **81**, 3108 (1998).
[10] M. Greiner, O. Mandel, T. Esslinger, T. W. Hänsch, and I. Bloch, Nature (London) **415**, 39 (2002).
[11] W. Zwerger, J. Opt. B **5**, S9 (2003).
[12] C. Orzel, A. K. Tuchman, M. L. Fenselau, M. Yasuda, and M. K. Kasevich, Science **291**, 2386 (2001).
[13] Z. Hadzibabic, S. Stock, B. Battelier, V. Bretin, and J. Dalibard, Phys. Rev. Lett. **93**, 180403 (2004).
[14] C. Schori, T. Stöferle, H. Moritz, M. Köhl, and T. Esslinger, Phys. Rev. Lett. **93**, 240402 (2004).
[15] V. A. Kashurnikov, N. V. Prokof'ev, and B. V. Svistunov, Phys. Rev. A **66**, 031601(R) (2002).
[16] R. Roth and K. Burnett, Phys. Rev. A **67**, 031602(R) (2003).
[17] C. Schroll, F. Marquardt, and C. Bruder, Phys. Rev. A **70**, 053609 (2004).
[18] T. Stöferle, H. Moritz, C. Schori, M. Köhl, and T. Esslinger, Phys. Rev. Lett. **92**, 130403 (2004).
[19] P. Pedri, L. Pitaevskii, S. Stringari, C. Fort, S. Burger, F. S. Cataliotti, P. Maddaloni, F. Minardi, and M. Inguscio, Phys. Rev. Lett. **87**, 220401 (2001).
[20] The value is obtained by averaging over $3 \times 3$ pixels around each position. We have checked that the visibility obtained this way was almost independent of the size of the integration region used to find $n_{max}$ and $n_{min}$.
[21] G. G. Batrouni, V. Rousseau, R. T. Scalettar, M. Rigol, A. Muramatsu, P. J. H. Denteneer, and M. Troyer, Phys. Rev. Lett. **89**, 117203 (2002).
[22] K. Sheshadri, H. R. Krishnamurthy, R. Pandit, and T. V. Ramakrishnan, Europhys. Lett. **22**, 257 (1993).
[23] D. van Oosten, P. van der Straten, and H. T. C. Stoof, Phys. Rev. A **63**, 053601 (2001).
[24] F. Schmitt, M. Hild, and R. Roth (private communication).
[25] P. Rabl, A. J. Daley, P. O. Fedichev, J. I. Cirac, and P. Zoller, Phys. Rev. Lett. **91**, 110403 (2003).
[26] G. Pupillo, A. M. Rey, G. Brennen, C. J. Williams, and C. W. Clark, J. Mod. Opt. **51**, 2395 (2004).
[27] B. DeMarco, C. Lannert, S. Vishveshwara, and T.-C. Wei, Phys. Rev. A **71**, 063601 (2005).
[28] D. M. Gangardt, P. Pedri, L. Santos, and G. V. Shlyapnikov, cond-mat/0408437.